Earthquakes and Structures, *Vol. 16, No. 1 (2019) 1-9*
DOI: https://doi.org/10.12989/eas.2019.16.1.001

Design theory and method of LNG isolation

Jiangang Sun[1a], Lifu Cui[*1], Xiang Li[1b], Zhen Wang[1a], Weibing Liu[1b] and Yuan Lv[2c]

[1]College of Civil Engineering, Dalian Minzu University, Dalian, China
[2]Institute of Road and Bridge Engineering, Dalian Maritime University, Dalian, China

(Received December 19, 2017, Revised October 18, 2018, Accepted November 22, 2018)

Abstract. To provide a simplified method for the base isolation design of LNG tanks, such as 16×104 m^3 LNG tanks, we conducted a derivation and calculation example analysis of the dynamic response of the base isolation of LNG storage tanks, using dynamic response analysis theory with consideration of pile-soil interaction. The ADINA finite element software package was used to conduct the numerical simulation analysis, and compare it with the theoretical solution. The ground-shaking table experiment of LNG tank base isolation was carried out simultaneously. The results show that the pile-soil interaction is not obvious under the condition of base isolation. Comparing base isolation to no isolation, the seismic response clearly decreases, but there is less of an effect on the shaking wave height after adopting pile top isolation support. This indicates that the basic isolation measures cannot control the wave height. A comparison of the shaking table experiment with the finite element solution and the theoretical solution shows that the finite element solution and theoretical solution are feasible. The three experiments are mutually verified.

Keywords: LNG storage tank; base isolation; pile-soil; vibration table experiment

1. Introduction

Large-scale earthquake disasters are a threat to LNG storage, as strong tremors result in structural damage and secondary disasters including fires and environmental pollution. The main difference between LNG and general equipment is that LNG contains cryogenic liquid. Thus, seismic and vibration issues are particularly problematic for LNG storage, and are research priorities. A large amount of research has been conducted, both domestically and globally. Research methodology focuses on theoretical analysis and numerical simulation, with little experimental research. Research considering soil and structural interaction is generally weak. To address the sparsity of high quality experimental research in this area, this paper considers the 16×10^4 m^3 LNG tank. Based on the basic theory of storage tank base isolation, the finite element numerical simulation analysis method, and the ground shaking table test of a simulated storage tank, we studied the LNG storage tank seismic response considering pile-soil interaction. The study provides theoretical, numerical, and experimental support for the isolation design of the LNG storage tank.

2. LNG storage tank isolation design theory considering pile-soil interaction

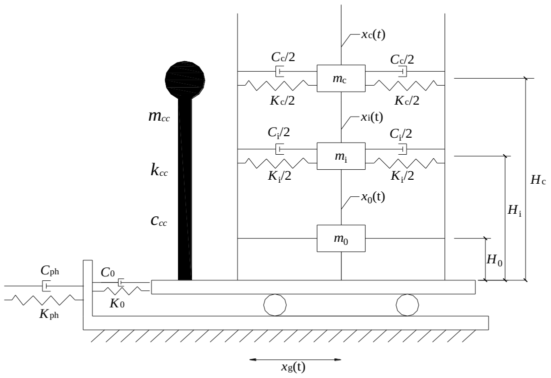

Fig. 1 The simplified analysis model of LNG storage tank isolation

2.1 Proposed simplified mechanical model

Simplifying the idea that the impact quality of the rigid wall theory is equivalent to the impact mass of the flexible wall theory, the seismic design of the tank for earthquake resistance considers the effect of convection mass. The mechanical model of the document is further simplified to the three-particle mechanical model shown in Fig. 1. Here, m_{cc}, m_c, m_i, and m_0 are the equivalent mass of the external tank particle, convective particle, impact particle and rigid particle, respectively. K_{cc}, K_c, and K_i are the equivalent stiffness of the external tank particle, the convection particle, and the impact particle, respectively. C_{cc}, C_c, and C_i are the equivalent damping of the external tank, the convection particle and the impact particle, respectively. H_c, H_i and H_0 are the equivalent height of the external tank, the convection particle, and the impact particle, respectively. The stiffness and the damping of the isolation layer are K_0

∗Corresponding author, Associate Professor
E-mail: fangzaijianzai@163.com
[a]Professor
[b]Postgraduate
[c]Ph.D. Student

http://www.techno-press.com/journals/eas&subpage=7
ISSN: 2092-7614 (Print), 2092-7622 (Online)

and C_0, respectively. The rigid pulse displacement is $x_0(t)$, the flexible pulse displacement is $x_i(t)$, the convective shaking displacement is $x_c(t)$, and the displacement of ground motion is $x_g(t)$.

2.2 Equations for LNG storage tank isolation design considering pile-soil interaction

1. Stiffness damping: The platform quality of the pile top is m_p, the horizontal stiffness of pile foundation is k_{ph}, and the damping of the pile foundation is c_{ph}. The isolation cycle is T_0; thus, the isolation base frequency is

$$\omega_0 = 2\pi / T_0 \tag{1}$$

The damping ratio of isolation is ξ_0; thus, the isolation stiffness k_0 and damping c_0 are

$$k_0 = \omega_0^2 \left(m_i + m_c + m_0 + m_p + m_{cc}\right) \tag{2}$$

$$c_0 = 2\xi_0 \omega_0 \left(m_i + m_c + m_0 + m_p + m_{cc}\right) \tag{3}$$

respectively. The convection sloshing damping ratio of the liquid is ξ_c =0.005. The damping ratio of the elastic pulse is ξ_i=0.02. The corresponding dampings are

$$c_c = 2\xi_c \omega_c m_c \tag{4}$$

$$c_i = 2\xi_i m_i \omega_i \tag{5}$$

2. Motion equation for considering the isolation system:
The quality matrix is

$$M = \begin{bmatrix} m_{cc} & 0 & 0 & m_{cc} & m_{cc} \\ 0 & m_c & 0 & m_c & m_c \\ 0 & 0 & m_i & m_i & m_i \\ m_{cc} & m_c & m_i & (m_{cc} + m_0 + m_i + m_c + m_p) & (m_{cc} + m_0 + m_i + m_c + m_p) \\ m_{cc} & m_c & m_i & (m_{cc} + m_0 + m_i + m_c + m_p) & (m_{cc} + m_0 + m_i + m_c + m_p) \end{bmatrix} \tag{6}$$

The damping matrix is

$$C = \begin{bmatrix} c_{cc} & 0 & 0 & 0 & 0 \\ 0 & c_c & 0 & 0 & 0 \\ 0 & 0 & c_i & 0 & 0 \\ 0 & 0 & 0 & c_0 & 0 \\ 0 & 0 & 0 & 0 & c_{ph} \end{bmatrix} \tag{7}$$

The stiffness matrix is

$$K = \begin{bmatrix} k_{cc} & 0 & 0 & 0 & 0 \\ 0 & k_c & 0 & 0 & 0 \\ 0 & 0 & k_i & 0 & 0 \\ 0 & 0 & 0 & k_0 & 0 \\ 0 & 0 & 0 & 0 & k_{ph} \end{bmatrix} \tag{8}$$

The displacement of the concrete outer tank, isolation layer, and pile cap is $x_{cc}(t)$, $x_0(t)$, and $x_{ph}(t)$, respectively.

According to the Hamilton principle of structural dynamics, the motion control equation is under seismic isolation

$$M\begin{Bmatrix} \ddot{x}_{cc} \\ \ddot{x}_c \\ \ddot{x}_i \\ \ddot{x}_0 \\ \ddot{x}_{ph} \end{Bmatrix} + C\begin{Bmatrix} \dot{x}_{cc} \\ \dot{x}_c \\ \dot{x}_i \\ \dot{x}_0 \\ \dot{x}_{ph} \end{Bmatrix} + K\begin{Bmatrix} x_{cc} \\ x_c \\ x_i \\ x_0 \\ x_{ph} \end{Bmatrix} = -\ddot{x}_g(t)\begin{Bmatrix} m_{cc} \\ m_c \\ m_i \\ (m_{cc} + m_0 + m_i + m_c + m_p) \\ (m_{cc} + m_0 + m_i + m_c + m_p) \end{Bmatrix} \tag{9}$$

The seismic action load vector is

$$\{F\} = \ddot{x}_g(t)\begin{Bmatrix} m_{cc} \\ m_c \\ m_i \\ (m_{cc} + m_0 + m_i + m_c + m_p) \\ (m_{cc} + m_0 + m_i + m_c + m_p) \end{Bmatrix} \tag{10}$$

3. Consider the calculation of displacement and internal force under seismic isolation.

The equivalent linear constitutive relation is used; the method is solved by the Wilson-θ method. θ takes the value 1.37.

The acceleration, velocity, and displacement vector is $\{\ddot{x}\}$, $\{\dot{x}\}$, and $\{x\}$, respectively.

The relative acceleration vector is $\begin{Bmatrix} \ddot{x}_{cc}(t) \\ \ddot{x}_c(t) \\ \ddot{x}_i(t) \\ \ddot{x}_0(t) \\ \ddot{x}_{ph}(t) \end{Bmatrix}$

The absolute acceleration vector is

$$\begin{Bmatrix} \ddot{X}_{cc}(t) \\ \ddot{X}_c(t) \\ \ddot{X}_i(t) \\ \ddot{X}_0(t) \\ \ddot{X}_{ph}(t) \end{Bmatrix} = \begin{Bmatrix} \ddot{x}_{cc}(t) + \ddot{x}_0(t) + \ddot{x}_{ph}(t) + \ddot{x}_g(t) \\ \ddot{x}_c(t) + \ddot{x}_0(t) + \ddot{x}_{ph}(t) + \ddot{x}_g(t) \\ \ddot{x}_i(t) + \ddot{x}_0(t) + \ddot{x}_{ph}(t) + \ddot{x}_g(t) \\ \ddot{x}_0(t) + \ddot{x}_{ph}(t) + \ddot{x}_g(t) \\ \ddot{x}_{ph}(t) + \ddot{x}_g(t) \end{Bmatrix} \tag{11}$$

The relative displacement vector is $\begin{Bmatrix} x_{cc}(t) \\ x_c(t) \\ x_i(t) \\ x_0(t) \\ x_{ph}(t) \end{Bmatrix}$.

The base shear formula excluding consideration of the external tank response is

$$Q_1 = -[m_c \cdot \ddot{X}_c(t) + m_i \cdot \ddot{X}_i(t) + (m_0 + m_p) \cdot \ddot{X}_0(t)] \tag{12}$$

Table 1 16×10^4 m^3 LNG storage tank related parameters

Mechanical model equivalent mass	Mass/ 10^7 kg	Effective height/m	Basic cycle /s	Damping ratio
External tank particle	1.717	39.689	0.1291	0.05
Flexible pulse particle	4.0235	15.828	0.5505	0.02
Convection particle	4.2203	20.337	9.7673	0.005

Table 2 Isolation LNG tank seismic response peak considering and not considering pile-soil interaction

Seismic response	Shear force of inner tank wall /10^6 N	Total shear/ 10^6 N	Overturning moment of inner tank wall /10^6 Nm	Total overturning moment /10^6 Nm	Shaking wave height/m
considering pile-soil	60.6	97.0	853	2591	0.6628
ignoring pile-soil	60.8	98.3	855	2613	0.6665

The base shear formula incorporating consideration of the external tank response is

$$Q = -[m_c \cdot \ddot{X}_c(t) + m_i \cdot \ddot{X}_i(t) + (m_0 + m_p) \cdot \ddot{X}_0(t) + m_{cc} \cdot \ddot{X}_{cc}(t)] \quad (13)$$

The bending moment that is bear the inner tank walls is

$$M_i = -[m_c \cdot \ddot{X}_c(t) \cdot h_c + m_i \cdot \ddot{X}_i(t) \cdot h_i + m_0 \cdot \ddot{X}_0(t) \cdot h_0] \quad (14)$$

The bending moment that is bear the concrete floor (pile caps) is

$$M = -[m_c \cdot \ddot{X}_c(t) \cdot h_c + m_i \cdot \ddot{X}_i(t) \cdot h_i{}' + m_0 \cdot \ddot{X}_0(t) \cdot h_0' + m_{cc} \cdot \ddot{X}_{cc}(t) \cdot (H + 1) + m_b \cdot \ddot{X}_0(t) \cdot 1] \quad (15)$$

The shaking wave height takes the smaller value in the following two types

$$h_{wv} = -(\frac{R \cdot (\ddot{x}_g(t) + \ddot{x}_0(t))}{g} + \frac{2R\ddot{x}_c(t)}{(1.84^2 - 1)g}) \quad (16)$$

$$h_{wv} = -\frac{0.837}{g}\{\ddot{x}_0(t) + \ddot{x}_g(t) + \ddot{x}_c(t) + \ddot{x}_{ph}(t)\}R \quad (17)$$

2.3 Sample analysis

The relevant parameters for a sample 16 × 10^4 m^3 LNG storage tank are listed in Table 1.

The horizontal seismic waves are selected such that the peak acceleration is 0.34 g at site Ⅲ, the isolation period is 2s, and the isolation layer damping ratio is 0.1. According to the pile foundation[10] standard, the horizontal stiffness of pile-soil interaction in k_{ph}=1.798×1010 N/m. The damping coefficient of the pile-soil interaction C_{ph}=6.018×107 Ns/m is as per site III. Aiming for a simplified mechanics model (Fig. 1), LNG tank seismic response analysis is conducted, under the following conditions: isolation; no isolation; ignoring pile-soil interaction; considering pile-soil interaction. Results are listed in Tables 2 and 3.

Table 3 Isolation and no isolation LNG tank seismic response peak and shock absorption rate considering pile-soil interaction

Seismic response	Shear force of inner tank wall /10^6N	Total shear/ 10^6N	Overturning moment of inner tank wall /10^6N·m	Total overturning moment /10^6N·m	Shaking wave height/m
no isolation	363.1	572.0	5750	15519	0.6425
isolation	60.8	98.3	855	2613	0.6665
shock absorption rate (%)	83.3	82.8	85.1	83.2	-3.7

Tables 2 and 3 indicate that the effect of pile-soil interaction is not obvious under base isolation. Contrasting base isolation with non-isolation, the total shear force of the base, shear force of inner tank wall, total overturning moment of the base, and overturning moment of inner tank wall are significantly reduced. The peak shock absorption rate ranges from 69% to 85%. The effect of damping on pile-soil interaction is achieved after the pile top isolation support is adopted, but there is little weakening effect on the wave height, indicating that the basic isolation measures cannot control the wave height. From a security point of view, the influence of pile-soil interaction on the tank was considered separately from the isolation design. The pile-soil interaction was not considered in the no isolation test. The effect of pile-soil interaction on the tank is considered when the isolation is designed.

3. Numerical analysis of seismic response of LNG storage tank considering pile-soil interaction

3.1 Model development and selection parameters

3.1.1 Geometric parameters of LNG tanks

The material parameters of LNG tank are as follows: the thickness of the outer tank wall is 0.8 m, height is 38.55 m, inner center radius of the outer tank wall is 41 m, edge thickness of the curved top is 0.8 m, thickness of the center plate is 0.4 m, thickness of the bottom plate is 0.9 m, thickness of the steel tank bottom is 24. 9 mm, reservoir height is 34.26 m, lining interval of the tank wall inside and outside is 1 m, and center diameter of the inner tank wall is 80 m. The height of the inner tank wall is 35.43 m, and this wall is sub-divided vertically into 10 rings. The length of the pile is 30 m. The specific material parameters are listed in Table 4.

3.1.2 Establishment and the selection of spring element parameters of the finite element model of pile-soil

To simplify the calculation, the pile foundation is simplified to Beam units in this paper, and the soil is

Table 4 Material parameters of LNG tank

Material	Parameters	Numerical
9% Ni steel	density/kg·m^{-3} elasticity modulus /N·mm^{-2} Poisson's ratio yield strength /MPa	7850 2.06×10^{11} 0.3 490
Prestressed concrete	density/kg·m^{-3} elasticity modulus /N·mm^{-2} Poisson's ratio	2500 3.45×10^{10} 0.17
Liquefied natural gas	density/kg·m^{-3} elasticity modulus /N·mm^{-2}	480 2.56×10^{9}

simplified to spring units. Because the foundation soil is stratified, the shape and parameters of each layer of soil comprising the pile foundation of the LNG storage tank differ. The stiffness coefficient of the soil is described by a specific non-rigorous numerical value. In order to calculate the equivalent stiffness and damping coefficient of stratified soil, the Pengjin model which considers the non-linear nature of the earth, recommended by the Japanese architectural society, is used. The soil calculation is simplified by using the mass-spring damper unit. This paper considers the proposed site soil according to the nature of each layer. The spring-damper unit is established from the value at the center of each Beam element. The stiffness coefficient K and the damping coefficient C of each layer soil are determined by the following

$$(K_h)_i=\begin{cases}0.5(K_h)_1H_i & i=1\\ 0.5\{(K_h)_{i-1}H_{i-1}+(K_h)_iH_i\} & i=2\sim N-1\\ 0.5(K_h)_{N-1}H_{N-1} & i-N\end{cases}\tag{18}$$

$$(c_h)_i=\begin{cases}0.5(c_h)_1H_i & i=1\\ 0.5\{(c_h)_{i-1}H_{i-1}+(c_h)_iH_i\} & i=2\sim N-1\\ 0.5(c_h)_{N-1}H_{N-1} & i-N\end{cases}\tag{19}$$

Based on the stress characteristics of pile foundation, the horizontal stiffness coefficient of single pile foundation, is calculated as *fe*

$$\left(K_{\mathrm{h}}\right)_{\mathrm{i}}=1.30\left(\frac{E_{\mathrm{si}}B^4}{E_{\mathrm{p}}I_{\mathrm{p}}}\right)^{\frac{1}{12}}\cdot\frac{E_{\mathrm{si}}}{\left(1-\mathrm{v}_{\mathrm{si}}^2\right)}\tag{20}$$

Gazetas puts forward to the equivalent damping coefficient of single pile weak soil which can be calculated by (21).

$$\left(\mathrm{c}_{\mathrm{h}}\right)_{\mathrm{i}}=2\rho_{\mathrm{si}}\left(V_{\mathrm{si}}+V_{L\mathrm{si}}\right)B\tag{21}$$

Randolph's study shows that the stiffness and damping of the pile vertical spring stiffness and friction damping are calculated by formulas (22) and (23).

$$\left(K_{\mathrm{s}}\right)_{\mathrm{i}}=\frac{2\pi G_{\mathrm{si}}}{\mathrm{In}\lfloor 5\mathrm{H}_{\mathrm{i}}\left(1-\mathrm{v/B}\right)\rfloor}\tag{22}$$

$$\mathrm{c}_{\mathrm{vsi}}=\rho_{\mathrm{si}}BV_{\mathrm{si}}+\frac{2\xi K_{\mathrm{si}}}{\omega}\tag{23}$$

Here, E_{si} is the elastic modulus of layer i soil, v_{si} is the Poisson's ratio of layer i soil, B is the diameter of the pile, E_p, I_p is the elastic modulus and section inertia of single pile, ρ_{si} is the density of soil on the pile side, V_{si} and VL_{si} are shear wave velocity, and tension and compression wave velocity, respectively, of layer I soil on the pile side. The damping coefficient of the soil is ξ, and ω is the remarkable cycle of ground soil.

3.1.3 Isolation layer parameters

In this study, the simulated isolation pedestal is calculated using an ordinary rubber bearing simulated by a spring element. Its natural vibration period is Tb=2s.

The equivalent viscous damping ratio is ζ=0.1. The stiffness coefficient of the spring K_b and the damping coefficient C_b are

$$K_b=m\cdot(\frac{2\pi}{T_b})^2\tag{24}$$

$$C_b=\zeta m\cdot\frac{4\pi}{T_b}\tag{25}$$

3.1.4 Unit selection

The finite element models of LNG storage tank that considers pile-soil interaction are shown in Fig. 2 and Fig. 3. The tank wall and concrete floor adopt 3D entity units, the inner tank wall adopts the four nodes Shell element, and the fluid adopts the FCBI fluid unit. The theory assumes that the liquid has no spin, heat transfer, viscosity, or micro-compressibility. With respect to fluid-solid coupling, the liquid surface is a free liquid surface. The pile foundation adopts the Beam element, the section size is the same as the actual project, and the number of the pile foundation are 360. The soil mass adopts the spring unit value, and the equivalent stiffness and damping are calculated according to the above formula.

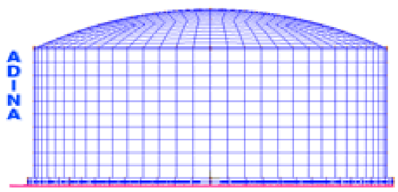

Fig. 2 No pile-soil LNG isolation tank

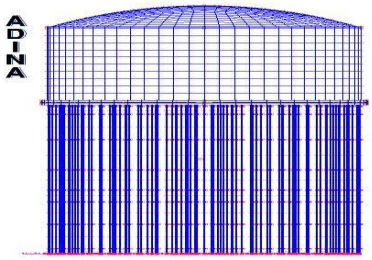

Fig. 3 The LNG isolation tank of 80 m pile foundation

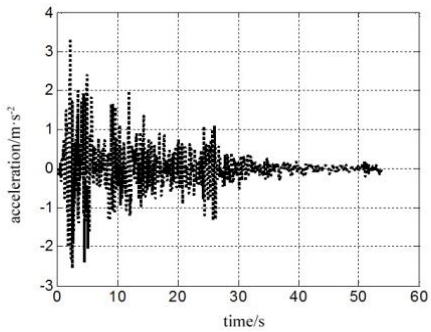

(a) The time history curve of El-centro wave

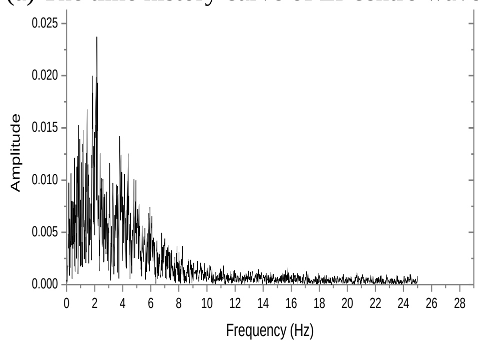

(b) The acceleration spectrum characteristics of El-centro wave

Fig. 4 The time history curve and spectrum characteristics of El-centro Seismic wave

3.2 Seismic input

The acceleration, g (9.8 m/s^2), is applied to the entire model. The damping ratio of the isolation layer is 0.1, and the isolation cycle is 2 s. The El-centro seismic wave is adopted according to the class III site protocol, the excellent frequency is 2.16 Hz, and the peak earthquake acceleration (PGA) is 0.34 g. The time history curve and spectrum characteristic of the El-centro seismic wave is shown in Fig. 4.

3.3 LNG isolation numerical simulation analysis considering pile-soil interaction under horizontal earthquake conditions

3.3.1 Numerical simulation comparison of analysis irrespective of pile-soil, and considering pile-soil

The El-centro wave is input, Peak ground acceleration is 0.34 g. The damping ratio of base isolation is 0.1, and the isolation period is 2 s. Using the models for considering pile-soil effect and disregarding pile-soil effect, numerical simulation of ADINA is performed. The results are listed in the table.

According to Table 5, the effect of pile-soil is not more obvious than the effect of base isolation under the base isolation condition. Therefore, considering the pile-soil effect can offer more accurate results under the base isolation condition. The peak stress of the steel inner pot is only 300 MPa; the 490 MPa 9% Ni steel yield strength is not reached, so the peak stress on the concrete outside the tank can be at most 3.8 MPa. This implies that the isolation design greatly improves the safety of the storage tank material.

Table 5 The peak comparison of pile-soil interaction effect under isolation under LNG tank isolation

Serial number	Described parameters	Unit	Disregarding pile-soil	Considering pile-soil	Rate of change
1	The acceleration peak of the internal tank	m/s^2	4.17	4.13	1.0
2	The acceleration peak of the external tank	m/s^2	3.81	3.74	1.8
3	The stress peak of internal tank	MPa	300.9	298.4	0.8
4	The stress peak of the external tank	MPa	3.32	3.37	-1.5
5	The peak of dynamic fluid pressure	kPa	19.9	15.9	20.1
6	The peak of shaking wave height	m	1.283	1.025	20.1
7	The peak of base shear	10^6 N	124.6	106.0	14.9
8	The peak of base moment	10^6 Nm	2776	2578	7.1

Table 6 Comparison of the base isolation effect of LNG tanks considering pile-soil

Serial number	Described parameters	Unit	No base isolation	Base isolation	Shock absorption rate
1	The acceleration peak of the internal tank	m/s^2	12.30	4.13	66.4
2	The acceleration peak of the external tank	m/s^2	6.68	3.74	44.0
3	The stress peak of internal tank	MPa	466.7	298.4	36.1
4	The stress peak of the external tank	MPa	3.73	3.37	9.7
5	The peak of dynamic fluid pressure	kPa	99.4	15.9	84.0
6	The peak of shaking wave height	m	0.891	1.025	-15.0
7	The peak of base shear	10^6N	482.0	106.0	78.0
8	The peak of base moment	10^6Nm	12082	2578	78.7

3.3.2 Analysis of base isolation effect considering the pile-soil effect

The El-centro wave is input, and peak ground acceleration is 0.34 g. The damping ratio of base isolation is 0.1, and the isolation period is 2 s. Numerical simulation of ADINA is performed using both the model that considers base isolation, and the model that disregards base isolation. The results are listed in the table.

According to Table 6, in addition to shaking wave height, the base isolation is still effective in reducing the seismic response when considering pile-soil effect. Therefore, base isolation is indispensable.

Table 7 The contrastive analysis of theoretical solutions and finite element solutions

Contrastive working condition	Calculated value	Contrasting the parameters		
		Total base shear /107N	Total base bending moment/10^9 Nm	Shaking wave height/m
Considering the pile-soil, no base isolation	Theoretical solution	57.20	15.519	0.643
	Finite element solution	48.20	12.082	0.891
	Error rate /%	15.7	22.1	27.8
Considering the pile-soil with base isolation	Theoretical solution	9.83	2.613	0.667
	Finite element solution	10.60	2.578	1.025
	Error rate /%	7.3	1.3	34.9

3.3.3 Analysis of theoretical solutions and finite element solutions

Considering two kinds of working condition data (the absence or presence of base isolation) with pile-soil interaction to verify the feasibility of solving equations, the finite element numerical simulation solution is compared with the theoretical solution. Results of this comparison are listed in Table 7.

As can be seen from Table 7, the orders of magnitude of the theoretical solution and the finite element solution are the same. The inner force is closer under base isolation, and the theoretical solution is small. Therefore, the internal force theory solution should be multiplied by a certain magnification factor in the design specification. The internal force deviation with base isolation is about 20%. The internal force theory solution is larger than the finite element solution, thus the adopted internal force theory solution is safe. The theoretical solution is less than the finite element solution for the shaking wave height, with or without base isolation. This is because when the theoretical solution is calculated, the shaking component only considers the first order mode component with a long period, whereas the finite element solution is a multi-order mode superposition. In addition, the theoretical solution ignores the contribution of the elastic vibration of the tank wall to the shaking component. It also results in a smaller shaking wave height. The theoretical solution for shaking wave height should be amplified to address this issue.

4 Analysis of rubber bearing base isolation test of the LNG inner tank

4.1 Test overview

According to both the mechanical and geometrical parameters of the earthquake simulation shaking table at Guangzhou university engineering structure seismic center, the parameters and values for the design test model (Fig. 5) should be as follows: diameter D_m=2.32 m, tank height L_m=2.12 m, elastic modulus of tank wall E_m=2.06×10^{11} N/m^2, Poisson’s ratio γ_m=0.3, density of tank wall ρ_{sm}=7.8 t/m^3, density of reservoir ρ_{Lm}=1.0 t/m^3, and wall thickness of tank h_{sm}=0.0012 m.

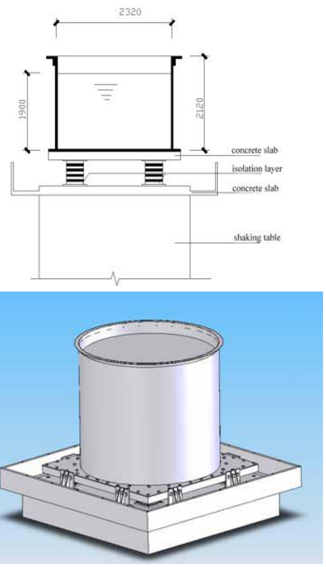

Fig. 5 The test model of the tank earthquake shaking table

(a) The tank model

(b) The physical model of the bottom board

(c) The physical model for isolation support

Fig. 6 The physical model of the storage tank

Three kinds of sensor are selected for use in the tank model earthquake shaking table test:

1) A displacement meter (test isolation layer, the displacement reaction of tank wall),

2) An accelerometer (test isolation layer, the acceleration reaction of tank wall), and

3) A liquid level meter (the reaction of liquid shaking wave height).

4.2 Selection of seismic waves

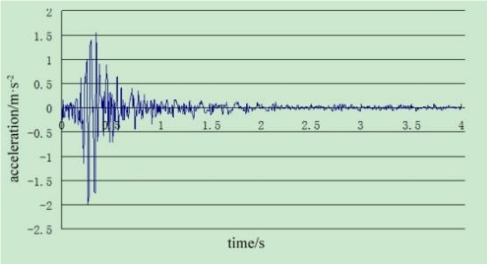

(a) The golden gate seismic waves

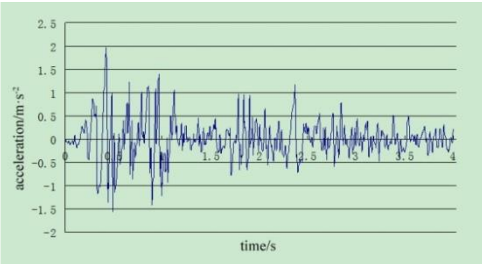

(b) Beijing diplomatic apartment seismic wave

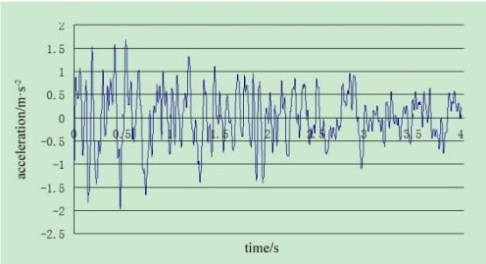

(c) El-centro seismic waves

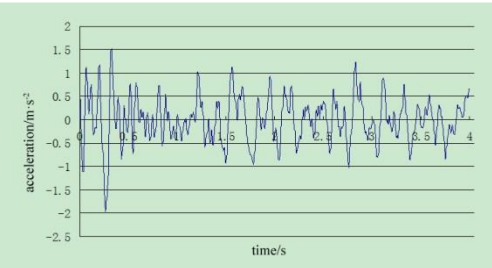

(d) Pasadena seismic wave

Fig. 7 Input seismic wave

4.3 Comparative analysis

The points along the height of the tank wall are 1~6. The tank wall acceleration response contrast figure of *X* direction isolation/lack of isolation are shown in Fig. 8, under one way seismic excitation and three-way seismic excitation.

Fig. 8 shows that the acceleration of tank wall has fallen more under one-way earthquake excitation. The isolation effect is obvious; in particular the tank wall liquid-solid coupling area clearly shows that acceleration has fallen sharply, and damping has been achieved. In addition to the golden gate seismic waves, the seismic effect of other seismic wave inputs is obviously reduced under three-way seismic excitation. In addition, three-way seismic excitation is compared with one-way earthquake excitation; here the acceleration response is clearly amplified, especially when horizontal base earthquake isolation is applied. The isolation seismic response of three-way seismic excitation is even greater than the seismic response of the one-way seismic excitation without isolation.

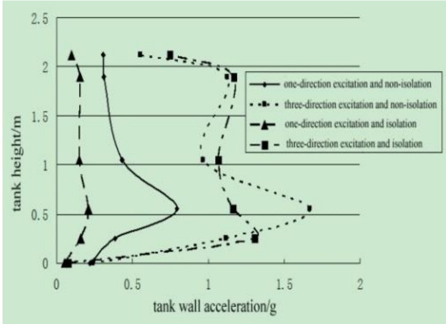

(a) The golden gate seismic waves

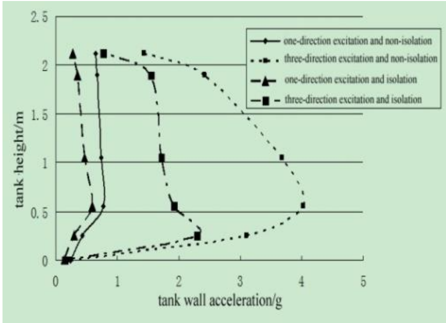

(b) Beijing diplomatic apartment seismic wave

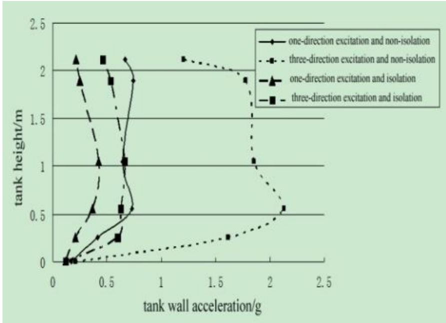

(c) El-centro seismic waves

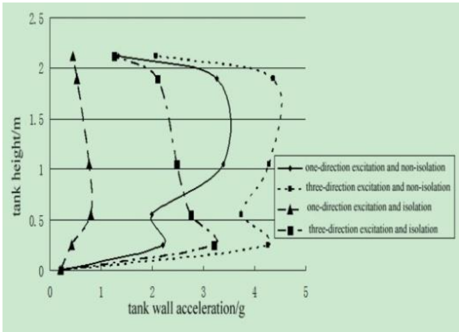

(d) Pasadena seismic wave

Fig. 8 The acceleration response without and with the isolation tank wall

Isolation stiffness is calculated through the hysteresis curve of isolation bearing and seismic displacement (0.608 mm, 2.68 mm, 1.888 mm, 4.816 mm) of the earthquake vibration table experiment. The base shear, shaking wave

Table 8 The comparison of theoretical solution and test solution of storage tank

Calculated value	Base shear			Shaking wave height /mm		
	Theoretical solution/N	Test solution /N	Difference rate/%	Theoretical solution /mm	Test solution /mm	Difference rate /%
Golden gate seismic waves	5283	5196	-1.67	6.89	15.59	55.81
Diplomatic apartment seismic wave	11912	10605	-12.32	16.83	19.97	15.72
El-centro seismic wave	12267	10343	-18.60	10.39	14.72	29.42
Pasadena seismic wave	23331	24927	6.40	15.35	18.45	16.80

Note: Difference rate=(test solution-theoretical solution)/ test solution×100%

Table 9 Comparison of the finite element solution and test solution for the storage tank

Calculated value	Base shear			Shaking wave height /mm		
	Theoretical solution/N	Test solution /N	Difference rate/%	Theoretical solution /mm	Test solution /mm	Difference rate /%
The golden gate seismic waves	5419	5196	-4.29	10.41	15.59	33.22
Diplomatic apartment seismic wave	12007.7	10605	-13.23	26.67	19.97	-33.55
El-centro seismic wave	14117.6	10343	-36.49	23.36	14.72	-58.70
Pasadena seismic wave	17997.5	24927	27.80	41.07	18.45	-55.08

Note: Difference rate=(test solution-theoretical solution)/ test solution × 100%

height, and the calculated value of theoretical analysis of the model tank earthquake vibration table experiment are listed in Table 8. The base shear, shaking wave height and the calculated value of finite element analysis of model tank earthquake vibration table experiment are listed in Table 9.

Table 8 shows that the base shear theoretical solution of the isolation tank differs less from the experimental solution with the input of different earthquakes' data. They are mutually validating. The calculation of the theoretical solution is feasible, but the shaking wave height is very different. The theoretical solution yields a lower value than the experimental solution, because the theoretical solution fails to consider the influence of the elastic deformation of the tank wall and the high-order mode of the reservoir. It is suggested that when the shaking wave height is calculated theoretically, the result must be adjusted to take this into account.

Table 9 shows that the base shear finite element solution of the isolation tank differs less from the experimental solution with the input of different earthquakes' data. The calculation of the theoretical solution is feasible, but the shaking wave height is very different.

The finite element solution yields a larger value than the experimental solution because, in addition to the golden gate seismic waves, the wave peak value is affected by hysteresis during the experiment. It is suggested that when the shaking wave height is calculated theoretically, the result must be adjusted to take this into account.

In addition, the difference in boundary conditions for the tank's bottom plate accounts for the differences between the experimental result, and the result of the theoretical and the finite element solutions.

The error of table-board input seismic oscillation, the defects of the tank itself and the installation error, etc.

5. Conclusions

This paper considers the pile-soil effect on a 16×10^4 m^3 LNG tank, using the basic theory of LNG isolation tanks, the finite element numerical simulation method, and the earthquake vibration table experimental method. The theory and method of isolation design of the LNG tank are studied. The main conclusions are as follows:

(1) Based on engineering design requirements, the simplified mechanical model and numerical simulation models of LNG storage tank isolation design, considering pile-soil effect, are established. The theory and method of LNG storage tank isolation design are given.

(2) The pile-soil interaction is not obvious under the condition of base isolation. Comparing results using base isolation with those when no isolation is used, the seismic response clearly decreases. However, decreased influence on the shaking wave height following the adoption of pile top isolation support, indicates that basic isolation measures cannot control the wave height.

(3) Comparing the shaking table experiment with the finite element solution and theoretical solution, shows that the finite element solution and theoretical solution are feasible, and the above three solutions are mutually verified.

Acknowledgements

Financial support, provided by the National Natural Science Foundation of China (No. 51078063, No. 51278089, and No. 51478090), and independent funding for scientific research projects funded by the central government (DC201502040403), is gratefully acknowledged.

References

API 620:2002 (2008), "Design and construction of large, welded, low-pressure storage tanks", American Petroleum Institute, 2002.JGJ 94-2008 Technical Code for Building Pile Foundation, China Architecture & Building Press, Beijing.

Colombo, J.I. and Almazán, J.L. (2017), "Experimental investigation on the seismic isolation for a legged wine storage tank", *J. Constr. Steel Res.*, **133**, 167-180.

Cui, L. (2008), "Research on the dynamic response analysis of three-dimensional seismic base isolation system of stand storage tanks", Daqing Petroleum Institute, Daqing. (in Chinese)

EN 14620:2006 (2007), "Design and manufacture of site built, vertical, cylindrical, flat-bottomed steel tanks for the storage of refrigerated, liquefied gases with operating temperatures between 0°C and -165°C", Europe.

GB 50011-2010 (2010), Code of Aseismic Design of Buildings, China Architecture & Building Press, Beijing.

Kalantari, A. (2017), "Seismic response reduction in liquid storage tanks by simple smart base isolation systems", *Iran. J. Sci. Technol. Tran. Civil Eng.*, **14**(2), 121-133.

Moeindarbari, H., Malekzadeh, M. and Taghikhany, T. (2014), "Probabilistic analysis of seismically isolated elevated liquid storage tank using multi-phase friction bearing", *Earthq. Struct.*, **6**(1), 111-125.

Saha, S.K., Matsagar, V.A. and Jain, A.K. (2015), "Reviewing dynamic analysis of base-isolated cylindrical liquid storage tanks under near-fault earthquakes", *IES J. Part A: Civil Struct. Eng.*, **8**(1), 41-61.

Saha, S.K., Matsagar, V.A. and Jain, A.K. (2016), "Seismic fragility of base-isolated water storage tanks under non-stationary earthquakes", *Bull. Earthq. Eng.*, **14**(4), 1153-1175.

Seleemah, A.A. and El-Sharkawy, M. (2011), "Seismic analysis and modeling of isolated elevated liquid storage tanks", *Earthq. Struct.*, **2**(4), 397-412.

Seleemah, A.A. and El-Sharkawy, M. (2011), "Seismic response of base isolated liquid storage ground tanks", *Ain Shams Eng. J.*, **2**(1), 33-42.

Shekari, M.R., Khaji, N. and Ahmadi, M.T. (2010), "On the seismic behavior of cylindrical base-isolated liquid storage tanks excited by long-period ground motions", *Soil Dyn. Earthq. Eng.*, **30**, 968-980.

Soni, D.P., Mistry, B.B. and Panchal, V.R. (2011), "Double variable frequency pendulum isolator for seismic isolation of liquid storage tanks", *Nucl. Eng. Des.*, **241**, 700-713.

Sun, J. (2009), *Isolation of Large Vertical Storage Tank-theory, Method, Test*, Science Press, Beijing. (in Chinese)

Sun, Y. (2012), "Seismic performance and isolation effective of large vertical liquid storage tank", Northeast Petroleum University, Daqing. (in Chinese)

Yang, Z.R., Shou, B.N., Sun, L. and Wang, J.J. (2011), "Earthquake response analysis of spherical tanks with seismic isolation", *Procedia Eng.*, **14**, 1879-1886.

Zou, D. (2012), "Study on non-linear seismic response of base-isolated liquid storage tanks with floating roof to bi-directional excitation", Northeast Petroleum University, Daqing. (in Chinese)

AT